Since January 2020 Elsevier has created a COVID-19 resource centre with free information in English and Mandarin on the novel coronavirus COVID-19. The COVID-19 resource centre is hosted on Elsevier Connect, the company's public news and information website.

Available online at www.sciencedirect.com

ScienceDirect

Journal of Nutritional Biochemistry 98 (2021) 108821

Journal of Nutritional Biochemistry

RESEARCH PAPER

Gut probiotic *Lactobacillus rhamnosus* attenuates PDE4B-mediated interleukin-6 induced by SARS-CoV-2 membrane glycoprotein

Minh Tan Pham[a,#], Albert Jackson Yang[a,#], Ming-Shan Kao[a], Uuganbayar Gankhuyag[a], Enkhbat Zayabaatar[a], Shiow-Lian Catherine Jin[b], Chun-Ming Huang[a,c,*]

[a] Department of Biomedical Sciences and Engineering, National Central University, Taoyuan, 32001, Taiwan
[b] Department of Life Sciences, National Central University, Taoyuan, 32001, Taiwan
[c] Department of Biomedical Science and Environmental Biology, Kaohsiung Medical University, Kaohsiung, 80708, Taiwan

Received 28 October 2020; received in revised form 30 April 2021; accepted 23 June 2021

Abstract

Membrane glycoprotein is the most abundant protein of severe acute respiratory syndrome coronavirus 2 (SARS-CoV-2), but its role in coronavirus disease 2019 (COVID-19) has not been fully characterized. Mice intranasally inoculated with membrane glycoprotein substantially increased the interleukin (IL)-6, a hallmark of the cytokine storm, in bronchoalveolar lavage fluid (BALF), compared to mice inoculated with green fluorescent protein (GFP). The high level of IL-6 induced by membrane glycoprotein was significantly diminished in phosphodiesterase 4 (PDE4B) knockout mice, demonstrating the essential role of PDE4B in IL-6 signaling. Mycelium fermentation of *Lactobacillus rhamnosus* (*L. rhamnosus*) EH8 strain yielded butyric acid, which can down-regulate the PDE4B expression and IL-6 secretion in macrophages. Feeding mice with mycelia increased the relative abundance of commensal *L. rhamnosus.* Two-week supplementation of mice with *L. rhamnosus* plus mycelia considerably decreased membrane glycoprotein-induced PDE4B expression and IL-6 secretion. The probiotic activity of *L. rhamnosus* plus mycelia against membrane glycoprotein was abolished in mice treated with GLPG-0974, an antagonist of free fatty acid receptor 2 (Ffar2). Activation of Ffar2 in the gut-lung axis for down-regulation of the PDE4B-IL-6 signalling may provide targets for development of modalities including probiotics for treatment of the cytokine storm in COVID-19.

Keywords: Cytokine storm; *Lactobacillus rhamnosus*; IL-6; PDE4B; SARS-CoV-2 membrane glycoprotein.

1. Introduction

Critical pneumonia in patients with coronavirus disease 2019 (COVID-19) can be associated with elevated inflammatory cytokines, a phenomenon known as a cytokine storm or macrophage activation syndrome (MAS) [1]. The hyper-induction of cytokines aggravated the auto-exaggerating inflammatory cascade, followed by multiple organ failure and lymphocytopenia, leading to dysregulated immunity [2]. In severe COVID-19 cases, the storm of interleukin-6 (IL)-6 can enhance the massive release of various inflammatory cytokines [3]. It has been documented that severe acute respiratory syndrome coronavirus (SARS-CoV) directly triggered IL-6 induction in human epithelial cells by binding to nuclear factor kappa-light-chain (NF-κB) of activated B cells and up-regulated gene expression of IL-6 [4]. Recent reports demonstrated that administration of phosphodiesterase 4 (PDE4) inhibitors, such as roflumilast with a higher affinity to PDE4B than PDE4A, C and D [5], acting on cyclic adenosine monophosphate (cAMP) pathway, represented a potential and effective therapy for COVID-19. Especially, PDE4 hydrolyzed cAMP to AMP by blocking cAMP hydrolysis, resulting in accumulating intracellular cAMP to positively regulate cytokine releases in macrophages [6].

Although there are many designated modalities such as corticosteroids, anti-viral or anti-malarial drugs to clinically control SARS-CoV-2, no evidence to date for the fully effective treatments to cure or alleviate the cytokine storm in COVID-19 patients [7]. While the number of COVID-19 positive cases is rapidly surging, the vaccine development has faced many challenges including the antigenic selection and drift, adverse effect, manufacture, and global distribution [8]. Therefore, an alternative approach may provide a great assistance in controlling the emergence of COVID-19 pandemic. The use of probiotic may propose a valuable solution against SARS-CoV-2 by generation of beneficial molecules to hinder the viral spread and suppress the massive inflammatory

* Corresponding author at: Chun-Ming Huang, Department of Biomedical Sciences and Engineering, National Central University, Taoyuan, 32001, Taiwan.
E-mail address: chunming@ncu.edu.tw (C.-M. Huang).
# Equally contributed.

https://doi.org/10.1016/j.jnutbio.2021.108821

responses [9]. Since the discovery of the gut-lung axis, evidence have revealed the advantages of probiotic bacteria to pulmonary health by delivering the fermentation metabolites to the lung via the bloodstream [10,11]. Short-chain fatty acids (SCFAs) such as butyric acid produced by gut probiotic can bind to free fatty acid receptors (Ffar) to dampen inflammation responses [12,13]. *Lactobacillus rhamnosus* (*L. rhamnosus*), a Gram-positive bacterium, is a commensal intestinal bacterial strain in mice and human [14]. Several studies have provided evidence for the protective role of lactic acid-producing bacteria in the defense against infections of viruses, including Ebola virus and cytomegalovirus [15]. *Lactobacillus paracasei* and *Lactobacillus plantarum* attenuated the secretion of pro-inflammatory IL-6 and IL-8 cytokines [16]. *L. rhamnosus* GG GR-1, and 4B15 strains substantially inhibited the release of tumor necrosis factor-alpha (TNF-α) in mouse macrophages [17,18]. Moreover, feeding mice with *Lactobacillus mucosae* or *fermentum* downregulated IL-6 and TNF-α in both acute and chronic inflammation [19].

In this study, we induced the fermentation of *L. rhamnosus* by the powder of mycelia, the vegetative part with high content of carbohydrates of a fungus [20], as a prebiotic. Our results demonstrated for the first time that the secretion of IL-6 and expression of PDE4B induced by SARS-CoV-2 membrane glycoprotein in the lung were considerably reduced when mice fed with *L. rhamnosus* plus fungal mycelia.

2. Materials and Methods

2.1. Ethics statement

Experiments of using Institute of Cancer Research (ICR) and PDE4B knockout mice [21] housed in an animal facility at National Central University (NCU) were conducted in accordance with a protocol (NCU-106-016, 19 December 2017) approved by the Institutional Animal Care and Use Committee (IACUC). ICR mice (female, 8-9 weeks old) were purchased from the National Laboratory Animal Center Taipei, Taiwan. Five mice per group were used in each experiment. Mice were sacrificed by CO_2 sedation in an encased chamber. The strain of *L. rhamnosus* EH8 stored in a Microbiome Bank in Professor Chun-Ming Huang's laboratory was originally isolated from human fecal samples according to a protocol (No. 19-013-B1, 22 May 2019) approved by the Institutional Review Board (IRB) at Landseed International Hospital, Taiwan. The sequenced nucleotides (Fig. S1) of 16S rRNA gene of *L. rhamnosus* EH8 shared 99.23% identity to those of *L. rhamnosus* 5681 (Genebank accession: MT463591.1).

2.2. Cloning, expression and purification of SARS-CoV-2 membrane glycoprotein

A plasmid carrying a gene encoding membrane glycoprotein (YP_009724393.1) of SARS-CoV-2 (Genebank accession: NC_045512.2) was transformed into *Escherichia coli* (*E. coli*) BL21 competent cells (Yeastern Biotech Co., Ltd, Taiwan). Transformation of a plasmid encoding green fluorescent protein (GFP) into *E. coli* BL21 served as a control. The *E. coli* BL21 Luria-Bertani (LB) broth (1 L) (Becton, Dickinson and Company, Franklin Lakes, NJ, USA) supplemented with 50 μg/mL kanamycin was cultivated to an optical density $(OD)_{600nm} = 0.6$. Proteins in *E. coli* BL21 were expressed by addition of 1 mM isopropyl β-D-thiogalactopyranoside (IPTG) at 20°C for 4 h, purified by a ProBond™ Purification System (Invitrogen, Carlsbad, CA, USA) and visualized in 10% sodium dodecyl sulfate-polyacrylamide gel electrophoresis (SDS-PAGE) gels stained by Coomassie Brilliant Blue R-250.

2.3. Detection of IL-6 in BALF

Recombinant proteins (100 μg) including SARS-CoV-2 membrane glycoprotein or GFP in phosphate buffered saline (PBS) (60 μL) were intranasally inoculated to mice. A small incision was made to insert a cannula into trachea. Bronchoalveolar lavage fluid (BALF) was collected by lavaging the lungs 3 times with 1 mL PBS 6 h after protein inoculation. The enzyme-linked immunosorbent assay (ELISA) using a Quantikine mouse IL-6 set (R&D Systems, Minneapolis, MN, USA) was carried out to quantified the level of IL-6 which was normalized to the concentration of total proteins in lung lavage.

2.4. Real-time polymerase chain reaction (RT PCR)

After intranasal inoculation of recombinant membrane glycoprotein or GFP, lung of ICR mice was homogenized in T-PER™ Tissue Protein Extraction Reagent (ThermoFisher Scientific, Waltham, MA, USA) supplemented with an ethylenediaminetetraacetic acid (EDTA)-free protease inhibitor cocktail (Sigma-Aldrich, St. Louis, MO, USA). RNA (1 ng) was converted into cDNA using an iScript cDNA Synthesis kit (Bio-Rad, Hercules, CA, USA). Primers were designed using the Primer-Blast tool from the National Center for Biotechnology Information (NCBI). The reaction of using cDNA (50 ng/μL) as a template was set for 40 cycles as follows: 95°C for 10 min followed by 95°C for 15 s, 60°C for 60 s, and 72°C for 30 s. A whole reaction was completed with 3 biological replicates, and each sample consisted of 3 technical replicates. The gene expression of GAPDH was used for normalization. The relative expression levels were analysed using the cycle threshold ($2^{-\Delta\Delta Ct}$) method. Primers for PDE4B and glyceraldehyde-3-phosphate dehydrogenase (GAPDH) were 5′GAACAAATG GGGCCTTAACA 3′ and reverse 5′ TTGTCCAGGAGGAGAACACC 3′; forward 5′ TGTGTCCGTCGTGGATCTGA 3′ and reverse 5′ GATGCCTGCTTCACCACCTT 3′, respectively.

2.5. Mycelium preparation

The inner portion of the basidiomata of *P. pulmonarius*, an oyster mushroom, was excised by a flamed scalpel blade under sterile conditions and placed onto on malt extract agar medium (MEA) (Scharlab, Barcelona, Spain) (Fig. S2A). Seven-day-old mycelium grown in the malt yeast peptone (MYP) broth [7 g/L malt extract (Scharlab), 1 g/L peptone (Amresco, Solon, Cleveland, USA) and 0.5 g/L yeast extract (ACE Biolabs, Amsterdam, Netherlands)] was harvested and homogenized with tissue grinders (Kimble Chase, Vineland, NJ, USA). The mycelium powder (Fig. S2B) was stored at 4°C.

2.6. Mycelium fermentation of L. rhamnosus EH8

L. rhamnosus [10^7 colony-forming unit (CFU) per mL, CFU/mL] was incubated in *Lactobacilli* MRS broth (55.15 g/L) (HiMedia Laboratories, Mumbai, India) in the absence or presence of 2% mycelium powder at 37°C for 24 h. MRS broth plus 2% mycelium powder without bacteria were incubated as a control. Phenol red [0.001% (w/v) (pH 7.4), Sigma-Aldrich] in MRS broth served as an indicator of fermentation, converting from red to orange-yellow when fermentation occurred. A colour change was detected by OD at 562 nm.

2.7. Quantification of L. rhamnosus

ICR mice were fed with 200 μl PBS or 2% mycelium powder in PBS daily. Two weeks after feeding, fecal was collected and dissolved 1:10 in 50 mM EDTA containing 5 mg lysozyme (Sigma-Aldrich). After centrifugation at 14,000 g for 2 min, DNA in the pellet was extracted by using a heat lysis protocol as described [22]. A StepOnePlus Real-time PCR System (ThermoFisher Scientific) using Power SYBR Green and PCR Master Mix (ThermoFisher Scientific) was used to quantify the abundance of *L. rhamnosus* in mouse feces. The reaction conditions of RT PCR was described above. Primers for *L. rhamnosus* detection were forward 5′ CGCCCTTAACAGCAGTCTTC 3′ and reverse 5′ GCCCTCCGTATGCTTAAACC 3′. Five mice per group were used in each experiment.

2.8. Cell culture

J774 macrophage cell lines (10^5 cells/well) were cultured in Dulbecco's Modified Eagle Medium (DMEM, ThermoFisher Scientific), 1% antibiotic (penicillin-streptomycin; 10,000 U/mL) (ThermoFisher Scientific), 25 mM Hepes and 10% fetal bovine serum (FBS) in 12-well cell culture plates (ThermoFisher Scientific). Cells were treated with 100 μM butyric acid or distilled H_2O (control) for 10 min before addition of 50 μg recombinant membrane glycoprotein at 37°C, 5% CO_2 for 12 h. In some experiments, cells were treated with 50 μg recombinant GFP or membrane glycoprotein. Three wells for each treatment were conducted. After centrifugation at 4,000 g for 5 min, the level of IL-6 in supernatants was quantified by ELISA. Cell pellets were extracted with a RNA mini kit (Ambion, Carlsbad, CA, USA). The gene expression of the PDE4B was quantified by RT PCR.

2.9. Detection of butyric acid by high performance liquid chromatography (HPLC)

L. rhamnosus EH8 (10^7 CFU/mL) was cultured in MRS broth in the presence or absence of 2% mycelium powder at 37°C for 24 h. Culture media were then collected and filtered through a 0.22 μm microfiltration membrane to remove bacteria and insoluble particles. Samples were added with the concentrated HCl (100 μL) and extracted for 20 min by gently rolling using 5 ml diethyl ether. After centrifugation at 3,500 rpm for 5 min, the supernatant was transferred to a Pyrex extraction tube before NaOH (500 μL of 1 mM) was added. The aqueous phase was moved to an autosampler vial and the concentrated HCl (100 μL) was added. The analysis of butyric acid in culture media was conducted using an Agilent 1200 series HPLC system with a ZORBAX Eclipse XDB-C18 column (4.6 × 250 mm, 5 μm). The mobile phase composed of 20 mmol/L NaH_2PO_4 solution (pH 2.2) and acetonitrile. The detector was set at 210 nm. The concentration of butyric acid was quantified according to a calibration curve of a butyric acid analytical standard.

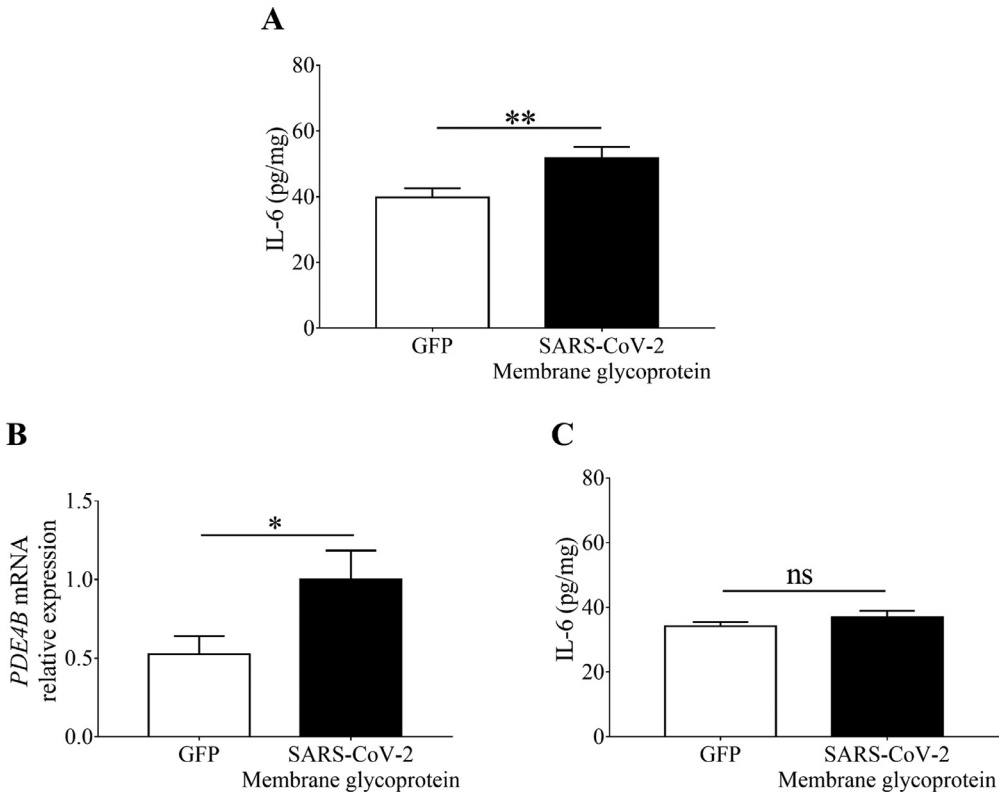

Fig. 1. Requirement of PDE4B for SARS-CoV-2 membrane glycoprotein-induced IL-6 in in the lung. (A) Recombinant SARS-CoV-2 membrane glycoprotein or GFP (100 μg/60μL PBS per mouse) was inoculated into the nasal cavities of ICR mice for 6 h. The level of IL-6 in BALF was measured by ELISA. (B) The relative expression of PDE4B mRNA in lung of SARS-CoV-2 membrane glycoprotein- or GFP-inoculated mice was detected by RT PCR. (C) The level of IL-6 in BALF was quantified in PDE4B knockout mice 6 h after intranasal inoculation of recombinant SARS-CoV-2 membrane glycoprotein or GFP. Data are the mean ± SD of experiments performed in triplicate. $^{*}p < 0.05$. $^{**}p < 0.01$. ns = non-significant (two-tailed *t*-test). Five mice per group were used in each experiment.

2.10. Inhibition of Ffar2

ICR mice (5 mice per group) were fed with *L. rhamnosus* EH8 (10^7 CFU) along with or without 2% mycelium powder at an interval of three days for 2 weeks. For Ffar2 inhibition, 200 μL of GLPG-0974 (5 μM), a Ffar2 antagonist, (Tocris Bioscience, Bristol, UK) was orally administrated every day for 3 days 10 min before mice were fed with *L. rhamnosus* EH8 in the presence or absence of mycelium powder. GLPG-0974 was dissolved in 5% DMSO (Sigma-Aldrich) in saline. Dimethyl sulfoxide (DMSO, 5% in saline) was used as a vehicle control for GLPG-0974. After two-week feeding of *L. rhamnosus* with or without mycelium powder, mice were nasally inoculated recombinant membrane glycoprotein (100 μg) for 6 h. The level of IL-6 in BALF was measured by ELISA.

2.11. Statistical analysis

GraphPad Prism® software was utilized for data analysis by unpaired t-test. The statistical significance was considered as: *P*-values of <0.05 (*), <0.01 (**), and <0.001 (***). The mean ± standard deviation (SD) was calculated from results obtained from at least three independent experiments.

3. Results

3.1. PDE4B is essential for induction of IL-6 by SARS-CoV-2 membrane glycoprotein

IL-6 is a chief component of excessive cytokines released by activated macrophages observed in severe COVID-19 patients [2,3]. The membrane glycoprotein (YP_009724393.1) of SARS-CoV-2 that caused COVID-19 was cloned into *E. coli* BL21 competent cells to obtain recombinant proteins. To examine the effect of SARS-CoV-2 membrane glycoprotein on the IL-6 production, we intranasally inoculated recombinant SARS-CoV-2 membrane glycoprotein or control GFP into ICR mice for 6 h. The level of IL-6 in BALF was detected by ELISA. As shown in Fig. 1A, the level (51.74 ± 1.96 pg/mg) of IL-6 in the mice inoculated with membrane glycoprotein was significantly higher than that (39.79 ± 1.60 pg/mg) in the mice inoculated with GFP. It has been shown that inhibition of PDE4 decreased the release of IL-6 in the lung [23]. The mRNA expression of PDE4B normalized with that of GAPDH in the lung was examined by RT PCR after inoculation of recombinant proteins. Relative to GFP, inoculation of SARS-CoV-2 membrane glycoprotein induced an approximately 2-fold increase in the mRNA expression of PDE4B (Fig. 1B). Furthermore, the increase in IL-6 secretion was completely suppressed when SARS-CoV-2 membrane glycoprotein was intranasally inoculated into the PDE4B knockout mice (Fig. 1C), suggesting that PDE4B plays an essential role in SARS-CoV-2 membrane glycoprotein-induced IL-6 secretion in the lung.

3.2. Mycelium fermentation of L. rhamnosus EH8 mitigates SARS-CoV-2 membrane glycoprotein-induced IL-6

Many natural extracts as prebiotics, containing high content of polysaccharides, can withstand digestion and absorption in the small intestine and can be selectively fermented by probiotic gut bacteria [24]. Mycelia, which are rich in polysaccharides, were isolated from *Pleurotus pulmonarius* (*P. pulmonarius*) [25]. To examine the prebiotic property of fungal mycelia, the *L. rhamnosus* EH8 [10^7 CFU], a commensal bacterial strain isolated from human faeces, was incubated in phenol red-containing *Lactobacilli* MRS broth in the presence of 2% mycelium powder under anaerobic conditions for 24 h. The incubation of mycelium powder alone or *L. rhamnosus* EH8 alone in MRS broth served as controls. The MRS broth incubating *L. rhamnosus* EH8 in the presence of mycelium pow-

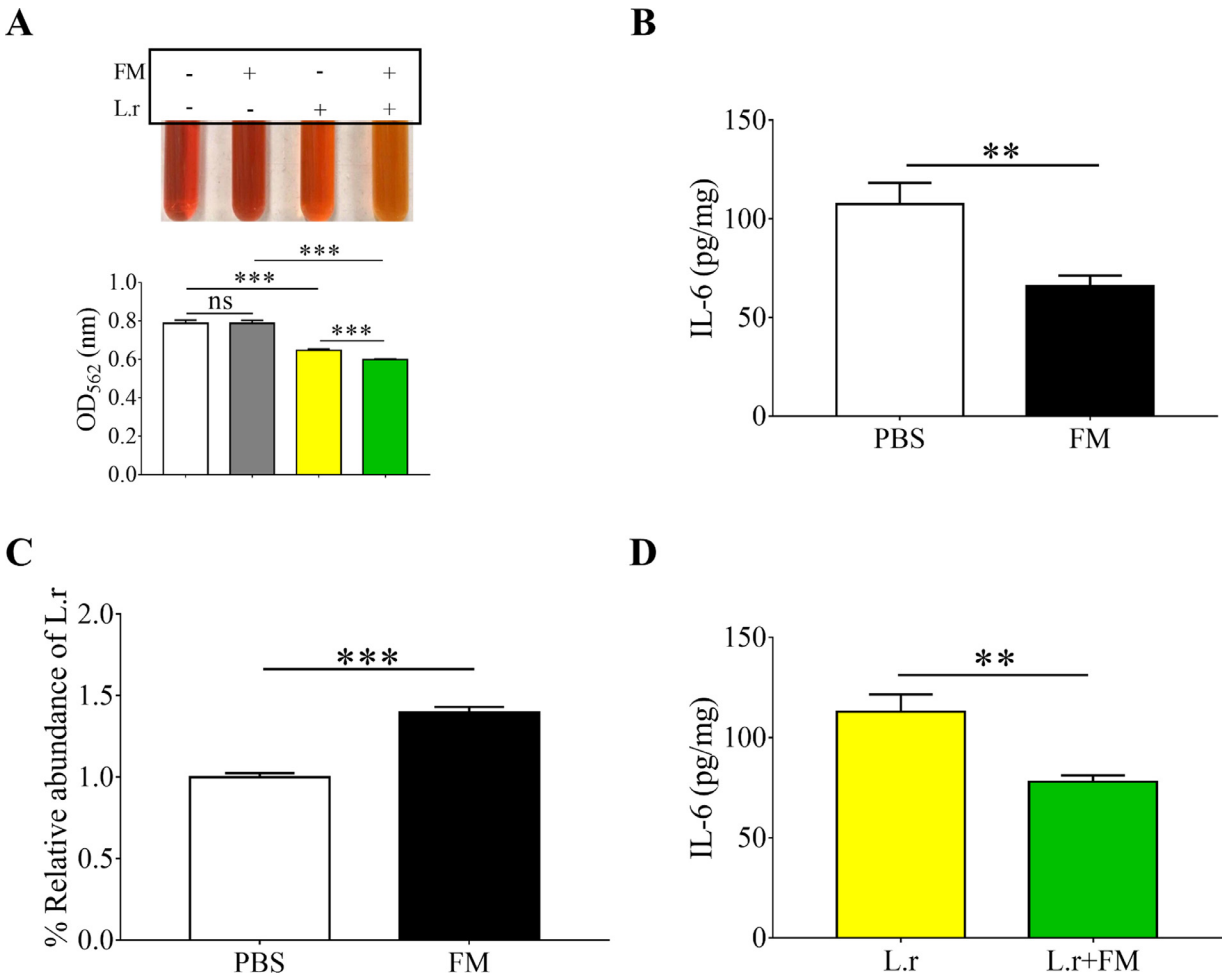

Fig. 2. Enhancement of *L. rhamnosus* abundance in the gut by mycelia and reduction of IL-6 in the lung by feeding mice with mycelia or *L. rhamnosus* EH8 plus mycelia. (A) *L. rhamnosus* EH8 (L.r) (10^7 CFU/mL) was incubated in MRS broth containing phenol red with or without 2% fungal mycelia (FM) for 24 h. Mycelium fermentation of *L. rhamnosus* EH8 was indicated by the colour change of phenol red to orange-yellow and a OD_{562} reduction. (B) ICR mice were fed with 2% fungal mycelia in PBS or the same volume of PBS. The levels of IL-6 in BALF were measured by ELISA. (C) The abundance of *L. rhamnosus* in facal samples analyzed by RT PCR after feeding with fungal mycelia or PBS. (D) The levels of IL-6 in BALF were quantified in ICR mice fed with *L. rhamnosus* EH8 in the presence (L.r+FM) or absence (L.r) of 2% fungal mycelia. Data are the mean ± SD of three independent experiments. $^{**}p < 0.01$. $^{***}p < 0.001$ (two-tailed *t*-test). Five mice per group were used in each experiment.

der, neither mycelium powder alone nor *L. rhamnosus* EH8 alone, turned orange-yellow and had OD_{562} reduction after incubation for 24 h, demonstrating the mycelium fermentation of *L. rhamnosus* EH8 (Fig. 2A).

Nasal inoculation of SARS-CoV-2 membrane glycoprotein into mice elevated IL-6 in the lung (Fig. 1A). To investigate the effect of mycelium powder on SARS-CoV-2 membrane glycoprotein-induced IL-6, mice were fed with mycelium powder or PBS every day for 2 weeks before intranasal inoculation of membrane glycoprotein for 6 h. As shown in Fig. 2B, feeding mice with mycelium powder, but not PBS, significantly diminished the SARS-CoV-2 membrane glycoprotein-induced IL-6 in BALF. *L. rhamnosus* can be detected in the murine gut microbiota [26]. To investigate if feeding mice with mycelium powder altered the abundance of *L. rhamnosus* in the gastrointestinal tract, the number of *L. rhamnosus* in mouse faeces collected 2 weeks after feeding was detected by RT PCR. Data in Fig. 2C demonstrated that the feeding mycelium powder resulted in an approximately 2-fold increase in the abundance of *L. rhamnosus*. Results in Fig. 2A-C suggested that mycelium powder may promote *L. rhamnosus* fermentation to reduce SARS-CoV-2 membrane glycoprotein-induced IL-6. We next fed mice with *L. rhamnosus* EH8 in the presence or absence of mycelium powder every day for 2 weeks. Feeding mice with *L. rhamnosus* EH8 plus mycelium powder markedly lowered the SARS-CoV-2 membrane glycoprotein-induced IL-6 in BALF compared to mice fed with *L. rhamnosus* EH8 alone (Fig. 2D).

3.3. Butyric acid was produced by mycelium fermentation of L. rhamnosus EH8 and reduced IL-6 secretion and PDE4B expression in macrophages

Since the anti-inflammatory property of butyric acid has been demonstrated [27], we measured the amounts of butyric acid in media of mycelium fermentation of *L. rhamnosus* EH8 by HPLC. The different concentrations (0-100 mM) of butyric acid were subjected to HPLC to establish a quantitative standard curve. Approximately 10 and 20 mM butyric acid were detected in the culture media of *L. rhamnosus* EH8 in the absence or presence of 2% mycelium powder (Fig. 3A), respectively, illustrating the prebiotic property of mycelium powder for *L. rhamnosus* EH8. In Fig. 1B, we demonstrated the up-regulation of PDE4B mRNA expression in the lung by SARS-CoV-2 membrane glycoprotein. Since, from four PDE4 isoforms, PDE4B is the only one expressed in macrophages [28], we cultured the J774 macrophages, a murine cell line that was widely

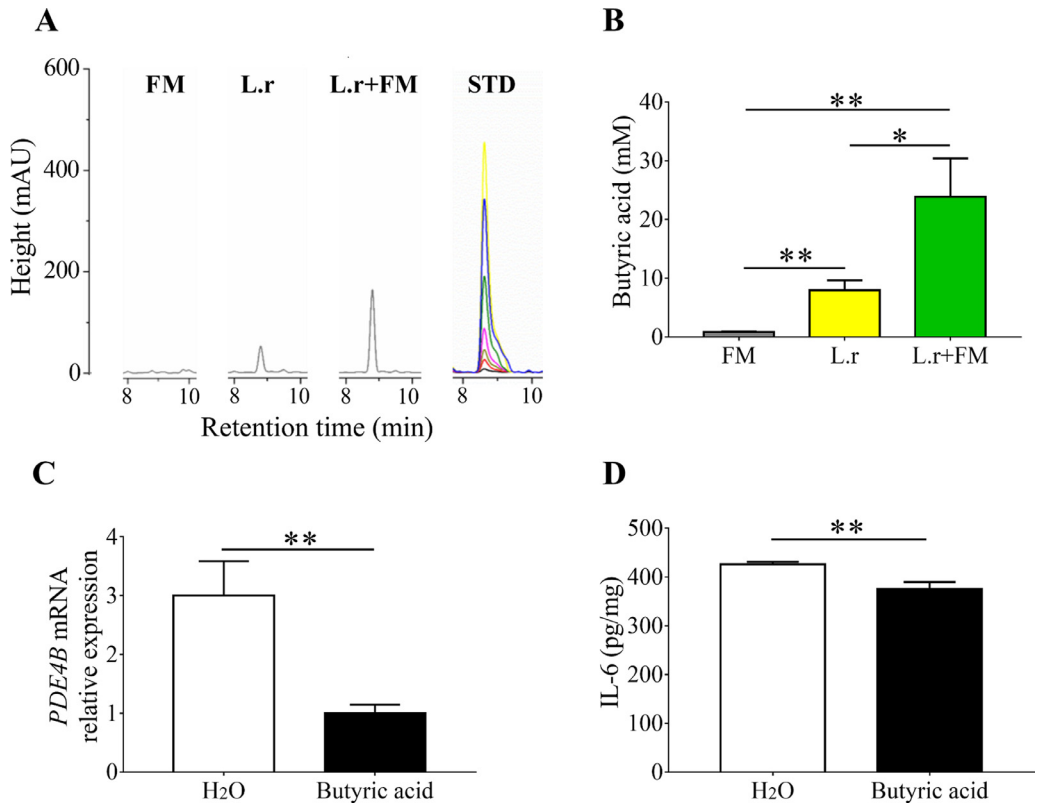

Fig. 3. Reduction of SARS-CoV-2 membrane glycoprotein-induced IL-6 secretion and PDE4B expression by butyric acid produced by mycelium fermentation of *L. rhamnosus* EH8. (A) HPLC chromatographs with milli-absorbance units (mAU) of the butyric acid in media containing mycelium (FM), *L. rhamnosus* EH8 (L.r) or *L. rhamnosus* EH8 plus mycelium (L.r+FM) were displayed. Different concentrations of butyric acid were applied onto HPLC to establish a standard curve (STD). (B) The concentrations of butyric acid were quantified based on the height (mAU) of STD. J774 macrophage cell lines (10^5 cells/well) in 12-well cell culture plates were treated with butyric acid or H_2O for 10 min before addition of SARS-CoV-2 membrane glycoprotein for 12 h. (C) The mRNA expression of PDE4B and (D) secretion of IL-6 were quantified by RT PCR and ELISA, respectively. Results are the mean ± SD obtained from three separate experiments. $^*p < 0.05$. $^{**}p < 0.01$ (two-tailed *t*-test).

used for studying of respiratory infection [29], to examine the effect of butyric acid on the PDE4 mRNA expression and IL-6 secretion. As shown in Fig. 3C, D, treatment of J774 macrophages with butyric acid, but H_2O significantly reduced SARS-CoV-2 membrane glycoprotein-induced PDE4B mRNA expression and IL-6 secretion.

3.4. Ffar2 mediates the effect of mycelium fermentation of L. rhamnosus EH8 on reduction of PDE4B and IL-6

Ffar2 has high affinity for butyric acid and is expressed by various cells including macrophages and epithelial cells in nasal cavities and lung [30]. To assess the engagement of Ffar2 on the effect of mycelium fermentation of *L. rhamnosus* EH8, GLPG-0974 in DMSO was given to mice to antagonize the Ffar2 before feeding mice with mycelium fermentation of *L. rhamnosus* EH8. Mice given DMSO served as a control. Two weeks after feeding mice with *L. rhamnosus* EH8 plus mycelium powder every day, mice were intranasally inoculated with SARS-CoV-2 membrane glycoprotein for 6 h. Compared to PDE4B mRNA expression in mice given DMSO control, mice given GLPG-0974 resulted in a substantial increase in the PDE4B expression in the lung (Fig. 4A). Similarly, treatment with GLPG-0974 significantly raised the level (8.44 ± 0.82 pg/mg) of IL-6 in BALF compared to IL-6 content (1.00 ± 0.25 pg/mg) in mice treated with control (Fig. 4B). Cumulatively, these data demonstrate that mycelium fermentation of *L. rhamnosus* EH8 required Ffar2 to weaken the aggravation of PDE4B mRNA expression and IL-6 secretion induced by SARS-CoV-2 membrane glycoprotein.

4. Discussion

The envelopes of coronaviruses, a group of positive-strand RNA viruses, contain three main proteins: the spike protein, membrane glycoprotein, and envelope protein. a non-glycosylated protein [31]. The RNA is packaged by the nucleocapsid protein into a helical nucleocapsid. SARS-CoV-2 enters host cells via binding of the spike protein to angiotensin-converting enzyme 2 (ACE2). The binding of spike protein to ACE2 can induce hyper-activation of NF-κB pathway, leading to the induction of a variety of pro-inflammatory cytokines, including IL-6, TNF-α, and chemokines [32]. Literature has revealed that nucleocapsid protein of SARS coronavirus HB can bind directly to the NF-κB recognition elements on the IL-6 promoter and regulate IL-6 expression [4]. It has been documented that SARS-CoV-2 membrane glycoprotein impeded the production of anti-viral type I and III interferon (IFN) cytokines by targeting the signalling mediated by retinoic acid-inducible gene I (RIG-I) and melanoma differentiation-associated gene 5 (MDA-5)[33]. The SARS-CoV-2 membrane glycoprotein interacted with the complex of RIG-I, mitochondrial antiviral signaling (MAVS), and TANK-binding kinase 1 (TBK1), blocking the phosphorylation, nuclear translocation, and activation of phosphorylated interferon regulatory factor 3 (IRF3), a transcription factor which can be translocated to the nucleus and activate genes encoding IFN [34] Although several coronavirus proteins may directly or indirectly regulate the IL-6 production, the relationship between SARS-CoV-2 membrane glycoprotein and the secretion of IL-6 has not elucidated. Results in Fig. 1 demonstrated that SARS-CoV-2

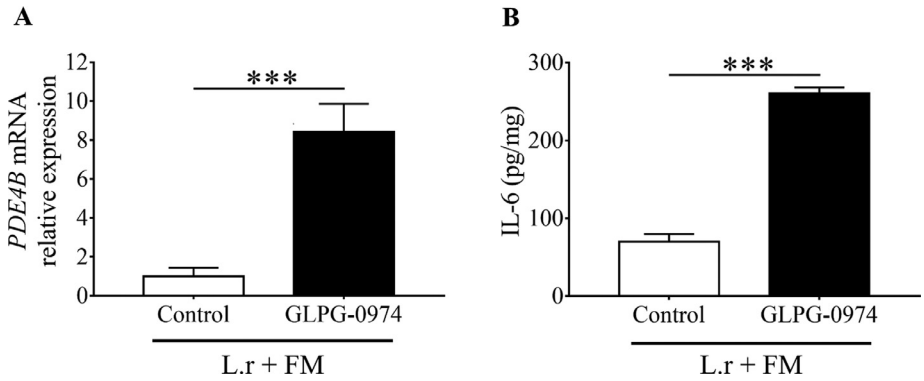

Fig. 4. Suppression of the action of *L. rhamnosus* EH8 plus mycelium to reduce the IL-6 and PDE4B by Ffar2 inhibition. ICR mice were given GLPG-0974, a Ffar2 antagonist, or its DMSO solvent as a control by gastric gavage every day for 3 days, then subsequently fed with *L. rhamnosus* EH8 plus fungal mycelium every day. Two weeks after feeding, mice were intranasally inoculated with SARS-CoV-2 membrane glycoprotein (100 μg/60μL PBS per mouse). The mRNA expression of PDE4B (A) and levels of IL-6 (B) in BALF were detected by RT PCR and ELISA, respectively. Data are the mean ± SD of experiments performed in triplicate. $^{***}p < 0.001$ (two-tailed *t*-test).

membrane glycoprotein can up-regulate the mRNA expression of PDE4B *in vivo*, one of four PDE4 isoforms expressed in macrophages[28]. Although many cells including macrophages and endothelial cells [35]in the respiratory system can produce IL-6, we demonstrated that SARS-CoV-2 membrane glycoprotein can increase the mRNA expression of PDE4B and trigger release of IL-6 from J774 macrophage cells (Fig. S3). Furthermore, the PDE4B is necessary for the secretion of IL-6 induced by membrane glycoprotein, since there is no difference in IL-6 content in PDE4B knockout mice intranasally inoculated with recombinant membrane glycoprotein or GFP. The result indicated that SARS-CoV-2 membrane glycoprotein may activate PDE4B to induce IL-6 secretion. Regulation of cAMP signalling by PDE4 to modulate the inflammatory responses in airway cells has been illustrated [36]. PDE4 inhibitor roflumilast has been approved as anti-inflammatory therapy [37]. Our results support the previous concept of using PDE4 inhibitors as potential drugs to target the cytokine storm in COVID-19 [6].

Although the clinical cut-off value for IL-6 as a biomarker for cytokine storm has not yet been determined, it has been reported that an IL-6 threshold greater than 80 pg/mL in sera carried prognostic value to predict respiratory failure COVID-19[38]. An IL-6 level above 100 pg/mL in sera of COVID-19 patients was found to correlate with mortality[39]. Although the process of collecting BALF dilutes the specimen, it is still unknown what real level of IL-6 in the lung can trigger a local cytokine storm. After normalization to the concentration of total proteins in lung lavage, the levels of IL-6 ranging from approximately 40 to 400 pg/mg in BALF of mice inoculated with SARS-CoV-2 membrane glycoprotein for 6 h were detected (Figs. 1-4). The fact of varying amounts of IL-6 in BALF were detected may be due to the differences in the molecules that were intranasally inoculated into mice. Cytokine storm can cause multiple-organ failure in COVID-19 infections[40]. Although inoculation with membrane glycoprotein for 6 h led to 23.1% higher level of IL-6 in BALF when compared to inoculation with GFP (Fig. 1A), cell death (55± 6%) in the lung inoculated with membrane glycoprotein was considerably higher than that (16± 3%) in the lung inoculated with GFP (Fig. S4). The result indicated that elevation of IL-6 may correlate with massive cell death and organ dysfunction.

The understanding of host-microbe cross-talk along the gut-lung axis highlights the significant role of SCFAs in shaping and promoting both innate and adaptive immunity in bone marrow to resolve airway inflammation [41]. Our results in Fig. 3 demonstrated that more than 20 mM butyric acid can be produced by the mycelium fermentation of *L. rhamnosus* EH8. Glucans in *P. pulmonarius* mycelium extracts exhibited the anti-inflammatory effect by blocking TNF-α-induced NF-κB nuclear translocation [42]. In addition, ACE inhibitory proteins have been identified in mycelium of *P. pulmonarius* [43]. Although glucose and galactose are prominent polysaccharides in fungal mycelium [44], it is not determined which carbon-rich molecules in *P. pulmonarius* mycelium act as prebiotics to induce the fermentation of *L. rhamnosus* EH8. Feeding mice with mycelium powders increased the relative abundance of *L. rhamnosus* in fecal samples (Fig. 2C). Augmentation of *L. rhamnosus* in mouse gut may explain why feeding mice with mycelium can suppress an elevation of IL-6 induced by SARS-CoV-2 membrane glycoprotein (Fig. 2B). Future studies will include the quantification of SCFAs in the gut after feeding mice with mycelium powders.

Studies are ongoing to test the notion of using probiotics to flatten the curve of COVID-2019 pandemic [45]. It has been reported that 3-60-day supplementation of probiotic *L rhamnosus* GG lowered the incidence of the respiratory tract infections of viruses by 2- to 3-fold compared to the placebo [46]. Inhibition of Ffar2 by GLPG-0974 dramatically blocked the action of *L. rhamnosus* EH8 plus mycelium to reduce SARS-CoV-2 membrane glycoprotein-induced PDE4B mRNA expression and IL-6 secretion (Fig. 4), demonstrating the essential role of Ffar2 in the probiotic activity of *L. rhamnosus* EH8 against the virulence of SARS-CoV-2 membrane glycoprotein. GLPG-0974 can be quickly absorbed with peak plasma concentrations reached between 2 and 4 h after oral administration in humans [47], indicating that oral administration of GLPG-0974 can effectively inhibit the Ffar2 in intestinal epithelium [48] and alveolar macrophages [49]. A knockout of Ffar2 which abundantly expressed on intestinal cells in mice exacerbated the colitis and intestinal inflammation [50]. Treatment with probiotic bacteria can upsurge the abundance of beneficial microbes and the levels of SCFAs including butyric acid, while down-regulating the production of pro-inflammatory IL-6 cytokine in aging mice [51]. Results from recent studies have demonstrated that sodium butyrate can suppress ACE2 expression in gut epithelial cells, alleviating the gastrointestinal inflammation associated with COVID-19[52]. Cytokine storm in COVID-19 is triggered by the release of IL-6 by alveolar macrophages [53]. Mycelium fermentation of *L. rhamnosus* EH8 yielded substantial amounts of butyric acid (Fig. 2A, B), which can lower both PDE4B mRNA expression and IL-6 secretion in J774 macrophage cell lines (Fig. 2C, D). Thus, it is worth investigating whether activation of Ffar2 on alveolar macrophages by butyric acid or its derivatives can efficiently inhibit the SARS-CoV-2 membrane glycoprotein-

induced IL-6 secretion. Inhibition of PDE4 increased intracellular cAMP and suppressed the release of pro-inflammatory cytokines [54]. We thus envision that PDE4B-mediated cAMP signalling in alveolar macrophages modulated the SARS-CoV-2 membrane glycoprotein-induced IL-6 secretion. The activation of signalling pathway of Ffar2, a G protein-coupled receptor (GPCR), to down-regulate the PDE4B is not yet characterized. However, it has been documented that members of the PDE4 family can interact with GPCRs- via β-arrestin proteins, which function as scaffolds to localize PDE4s to ligand-activated GPCRs [55].

Overall, although further research is needed to clarify how Ffar2 on alveolar macrophages can regulate the PDE4B-mediated cAMP signalling to calm the cytokine storm in COVID-19, our data demonstrated for the first time that PDE4B is an essential molecule that contributes to the SARS-CoV-2 membrane glycoprotein-induced IL-6 secretion. Mycelium fermentation of probiotic *L. rhamnosus* EH8 mediated Ffar2 to counteract the SARS-CoV-2 membrane glycoprotein, which elevated the PDE4B mRNA expression and IL-6 secretion in the lung.

Author Statement

Chun-Ming Huang: Conceptualization, Methodology, Supervision, Writing-Reviewing and Editing, Minh Tan Pham: Writing-Original draft preparation and experimental conduction, *Albert Jackson Yang:* Mouse maintenance and experiments, Min-Shan Kao: Gene cloning and protein expression, *Uuganbayar Gankhuyag:* Fungal extract preparation, Enkhbat Zayabaatar: in vitro cell culture, *Shiow-Lian Catherine Jin:* Knockout mouse breeding.

Funding

The study was supported by the Ministry of Science and Technology (MOST) Grants (108-2622-B-008-001-CC1; 108-2314-B-008-003-MY3, and 107-2923-B-008-001-MY3) and 106/107/108-Landseed Hospital-NCU joint grants.

Competing Interest

The authors declare no conflict of interest.

Acknowledgments

We especially thank Professor Ming-Fa Hsieh at the Department of Biomedical Engineering, Chung Yuan Christian University, Taoyuan, Taiwan, for his assistance at HPLC analysis. We also thank Syifa Labibah, Nguyen Mai Trinh Tang, Arun Balasubramaniam, and Shinta Marito for protein purification and cell culture.

Supplementary materials

Supplementary material associated with this article can be found, in the online version, at doi:10.1016/j.jnutbio.2021.108821.

References

[1] Song P, Li W, Xie J, Hou Y, You C. Cytokine storm induced by SARS-CoV-2. Clin Chim Acta 2020;509:280–7.
[2] Liu B, Li M, Zhou Z, Guan X, Xiang Y. Can we use interleukin-6 (IL-6) blockade for coronavirus disease 2019 (COVID-19)-induced cytokine release syndrome (CRS)? J Autoimmun 2020:102452.
[3] Liu T, Zhang J, Yang Y, Zhang L, Ma H, Li Z, et al. The potential role of IL-6 in monitoring coronavirus disease 2019. Available at SSRN 3548761 2020.
[4] Zhang X, Wu K, Wang D, Yue X, Song D, Zhu Y, et al. Nucleocapsid protein of SARS-CoV activates interleukin-6 expression through cellular transcription factor NF-κB. Virol 2007;365:324–35.
[5] Kawamatawong T. Roles of roflumilast, a selective phosphodiesterase 4 inhibitor, in airway diseases. J Thorac Dis 2017;9:1144.
[6] Dalamaga M, Karampela I, Mantzoros CS. Commentary: Phosphodiesterase 4 inhibitors as potential adjunct treatment targeting the cytokine storm in COVID-19. Metabolism 2020:154282.
[7] Mostafa T. Could oral PDE-5 inhibitors have a potential adjuvant role in combating COVID-19 infection? Sex Med Rev 2020.
[8] Shin MD, Shukla S, Chung YH, Beiss V, Chan SK, Ortega-Rivera OA, et al. COVID-19 vaccine development and a potential nanomaterial path forward. Nat Nanotechnol 2020;15:646–55.
[9] Chai W, Burwinkel M, Wang Z, Palissa C, Esch B, Twardziok S, et al. Antiviral effects of a probiotic *Enterococcus faecium* strain against transmissible gastroenteritis coronavirus. Arch Virol 2013;158:799–807.
[10] Dumas A, Bernard L, Poquet Y, Lugo-Villarino G, Neyrolles O. The role of the lung microbiota and the gut-lung axis in respiratory infectious diseases. Cell Microbiol 2018;20:e12966.
[11] Dickson RP. The microbiome and critical illness. Lancet Respir Med 2016;4:59–72.
[12] Rooks MG, Garrett WS. Gut microbiota, metabolites and host immunity. Nat Rev Immunol 2016;16:341–52.
[13] Jia W, Xie G, Jia W. Bile acid–microbiota crosstalk in gastrointestinal inflammation and carcinogenesis. Nat Rev Gastroenterol Hepatol 2018;15:111.
[14] Satokari R, Grönroos T, Laitinen K, Salminen S, Isolauri E. *Bifidobacterium* and *Lactobacillus* DNA in the human placenta. Lett Appl Microbiol 2009;48:8–12.
[15] Akour A. Probiotics and COVID-19: is there any link? Lett Appl Microbiol 2020;71:229–34.
[16] Schmitter T, Fiebich BL, Fischer JT, Gajfulin M, Larsson N, Rose T, et al. Ex vivo anti-inflammatory effects of probiotics for periodontal health. J Oral Microbiol 2018;10:1502027.
[17] Kim SO, Sheikh HI, Ha SD, Martins A, Reid G. G-CSF-mediated inhibition of JNK is a key mechanism for *Lactobacillus rhamnosus*-induced suppression of TNF production in macrophages. Cell Microbiol 2006;8:1958–71.
[18] Oh NS, Joung JY, Lee JY, Kim Y. Probiotic and anti-inflammatory potential of *Lactobacillus rhamnosus* 4B15 and *Lactobacillus gasseri* 4M13 isolated from infant feces. PloS one 2018;13:e0192021.
[19] Ayyanna R, Ankaiah D, Arul V. Anti-inflammatory and antioxidant properties of probiotic bacterium *Lactobacillus mucosae* AN1 and *Lactobacillus fermentum* SNR1 in Wistar albino rats. Front Microbiol 2018;9:3063.
[20] Aida F, Shuhaimi M, Yazid M, Maaruf A. Mushroom as a potential source of prebiotics: a review. Trends Food Sci Technol 2009;20:567–75.
[21] In: Jin S-LC, Latour AM, Conti M. Generation of PDE4 knockout mice by gene targeting. In: Lugnier C, editor. Phosphodiesterase methods and protocols Humana Press; 2005. p. 191–210.
[22] Martzy R, Bica-Schröder K, Pálvölgyi ÁM, Kolm C, Jakwerth S, Kirschner AK, et al. Simple lysis of bacterial cells for DNA-based diagnostics using hydrophilic ionic liquids. Sci Rep 2019;9:1–10.
[23] Kosutova P, Mikolka P, Kolomaznik M, Balentova S, Calkovska A, Mokra D. Effect of phosphodiesterase-4 inhibitor on the inflammation, oxidative damage and apoptosis in a saline lavage-induced model of acute lung injury. Eur Respiratory J 2018;52:PA5252.
[24] Liu Y, Wang C, Li J, Li T, Zhang Y, Liang Y, et al. *Phellinus linteus* polysaccharide extract improves insulin resistance by regulating gut microbiota composition. The FASEB J 2020;34:1065–78.
[25] Smiderle F, Olsen L, Ruthes A, Czelusniak P, Santana-Filho A, Sassaki G, et al. Exopolysaccharides, proteins and lipids in *Pleurotus pulmonarius* submerged culture using different carbon sources. Carbohydr Polym 2012;87:368–76.
[26] Chen P, Torralba M, Tan J, Embree M, Zengler K, Stärkel P, et al. Supplementation of saturated long-chain fatty acids maintains intestinal eubiosis and reduces ethanol-induced liver injury in mice. Gastroenterology 2015;148:203–14 e16.
[27] Traisaeng S, Batsukh A, Chuang T-H, Herr DR, Huang Y-F, Chimeddorj B, et al. *Leuconostoc mesenteroides* fermentation produces butyric acid and mediates Ffar2 to regulate blood glucose and insulin in type 1 diabetic mice. Sci Rep 2020;10:1–10.
[28] Yang J-X, Hsieh K-C, Chen Y-L, Lee C-K, Conti M, Chuang T-H, et al. Phosphodiesterase 4B negatively regulates endotoxin-activated interleukin-1 receptor antagonist responses in macrophages. Sci Rep 2017;7:1–13.
[29] Lowy RJ, Dimitrov DS. Characterization of influenza virus-induced death of J774. 1 macrophages. Exp Cell Res 1997;234:249–58.
[30] Wang G, Jiang L, Wang J, Zhang J, Kong F, Li Q, et al. The G protein-coupled receptor FFAR2 promotes internalization during influenza A virus entry. J Virol 2020;94.
[31] Ujike M, Taguchi F. Incorporation of spike and membrane glycoproteins into coronavirus virions. Viruses 2015;7:1700–25.
[32] Hirano T, Murakami M. COVID-19: A new virus, but a familiar receptor and cytokine release syndrome. Immunity 2020;52:731–3.
[33] Zheng Y, Zhuang MW, Han L, Zhang J, Nan ML, Zhan P, et al. Severe acute respiratory syndrome coronavirus 2 (SARS-CoV-2) membrane (M) protein inhibits type I and III interferon production by targeting RIG-I/MDA-5 signaling. Signal Transduct Target Ther 2020;5:299.
[34] Park A, Iwasaki A. Type I and Type III Interferons - Induction, Signaling, Evasion, and Application to Combat COVID-19. Cell Host Microbe 2020;27:870–8.
[35] Jirik FR, Podor TJ, Hirano T, Kishimoto T, Loskutoff DJ, Carson DA, Lotz M. Bacterial lipopolysaccharide and inflammatory mediators augment IL6 secretion by human endothelial cells. J Immunol 1989;142:144–7.

[36] Trian T, Burgess JK, Niimi K, Moir LM, Ge Q, Berger P, et al. β 2-Agonist induced cAMP is decreased in asthmatic airway smooth muscle due to increased PDE4D. PloS one 2011;6:e20000.
[37] Van Ly D, De Pedro M, James P, Morgan L, Black JL, Burgess JK, et al. Inhibition of phosphodiesterase 4 modulates cytokine induction from toll like receptor activated, but not rhinovirus infected, primary human airway smooth muscle. Respir Res 2013;14:127.
[38] Copaescu A, Smibert O, Gibson A, Phillips EJ, Trubiano JA. The role of IL-6 and other mediators in the cytokine storm associated with SARS-CoV-2 infection. J Allergy Clin Immunol 2020;146:518–34 e1.
[39] Chen LYC, Hoiland RL, Stukas S, Wellington CL, Sekhon MS. Confronting the controversy: interleukin-6 and the COVID-19 cytokine storm syndrome. Eur Respir J 2020;56:2003006.
[40] Iwasaki M, Saito J, Zhao H, Sakamoto A, Hirota K, Ma D. Inflammation Triggered by SARS-CoV-2 and ACE2 Augment Drives Multiple Organ Failure of Severe COVID-19: Molecular Mechanisms and Implications. Inflammation 2021;44:13–34.
[41] Dang AT, Marsland BJ. Microbes, metabolites, and the gut–lung axis. Mucosal Immunol 2019;12:843–50.
[42] Lavi I, Nimri L, Levinson D, Peri I, Hadar Y, Schwartz B. Glucans from the edible mushroom *Pleurotus pulmonarius* inhibit colitis-associated colon carcinogenesis in mice. J Gastroenterol 2012;47:504–18.
[43] Ibadallah BX, Abdullah N, Shuib AS. Identification of angiotensin-converting enzyme inhibitory proteins from mycelium of. Planta Med 2015;81:123–9.
[44] Lavi I, Levinson D, Peri I, Tekoah Y, Hadar Y, Schwartz B. Chemical characterization, antiproliferative and antiadhesive properties of polysaccharides extracted from *Pleurotus pulmonarius* mycelium and fruiting bodies. Appl Microbiol Biotechnol 2010;85:1977–90.
[45] Baud D, Agri VD, Gibson GR, Reid G, Giannoni E. Using probiotics to flatten the curve of coronavirus disease COVID-2019 pandemic. Front Public Health 2020;8:186.
[46] Luoto R, Ruuskanen O, Waris M, Kalliomäki M, Salminen S, Isolauri E. Prebiotic and probiotic supplementation prevents rhinovirus infections in preterm infants: a randomized, placebo-controlled trial. J Allergy Clin Immunol 2014;133:405–13.
[47] Namour F, Galien R, Van Kaem T, Van der Aa A, Vanhoutte F, Beetens J, et al. Safety, pharmacokinetics and pharmacodynamics of GLPG0974, a potent and selective FFA2 antagonist, in healthy male subjects. Br J Clin Pharmacol 2016;82:139–48.
[48] Sivaprakasam S, Gurav A, Paschall A, Coe G, Chaudhary K, Cai Y, et al. An essential role of Ffar2 (Gpr43) in dietary fibre-mediated promotion of healthy composition of gut microbiota and suppression of intestinal carcinogenesis. Oncogenesis 2016;5 e238-e.
[49] Liu Q, Tian X, Maruyama D, Arjomandi M, Prakash A. Lung immune tone regulation by the gut-lung immune axis: Short-chain fatty acid receptors FFAR2 and FFAR3, and IL-1β expression profiling in mouse and human lung. bioRxiv 2020.
[50] Masui R, Sasaki M, Funaki Y, Ogasawara N, Mizuno M, Iida A, et al. G protein–coupled receptor 43 moderates gut inflammation through cytokine regulation from mononuclear cells. Inflamm Bowel Dis 2013;19:2848–56.
[51] Vemuri R, Gundamaraju R, Shinde T, Perera AP, Basheer W, Southam B, et al. Lactobacillus acidophilus DDS-1 Modulates Intestinal-Specific Microbiota, Short-Chain Fatty Acid and Immunological Profiles in Aging Mice. Nutrients 2019;11:1297.
[52] Takahashi Y, Hayakawa A, Sano R, Fukuda H, Harada M, Kubo R, et al. Histone deacetylase inhibitors suppress ACE2 and ABO simultaneously, suggesting a preventive potential against COVID-19. Sci Rep 2021;11:3379.
[53] Wang C, Xie J, Zhao L, Fei X, Zhang H, Tan Y, et al. Aveolar macrophage activation and cytokine storm in the pathogenesis of severe COVID-19. Research Square 2020 March 25. doi:10.21203/rs.3.rs-19346/v1.
[54] Perez-Aso M, Montesinos MC, Mediero A, Wilder T, Schafer PH, Cronstein B. Apremilast, a novel phosphodiesterase 4 (PDE4) inhibitor, regulates inflammation through multiple cAMP downstream effectors. Arthritis Res Ther 2015;17:1–13.
[55] Vagena E, Ryu JK, Baeza-Raja B, Walsh NM, Syme C, Day JP, et al. A high-fat diet promotes depression-like behavior in mice by suppressing hypothalamic PKA signaling. Transl Psychiatry 2019;9:1–15.